


Cite this: *RSC Adv.*, 2024, 14, 21553

# Synthesis, characterization, and antibacterial activity of novel bis(indolyl)methanes sourced from biorenewable furfurals using gluconic acid aqueous solution (GAAS) as a sustainable catalyst†

Prajwal Naik C.,<sup>a</sup> Ashoka G. B.,<sup>b</sup> Asiful H. Seikh<sup>c</sup> and Saikat Dutta<sup>✉</sup><sup>\*,a</sup>

Bis(indolyl)methanes (BIMs) are important heterocycle-containing molecular scaffolds that show remarkable biological and pharmacological activities. This work reports the synthesis of novel BIMs using carbohydrate-derived 5-substituted-2-furaldehydes as renewable reactants. Structural diversity was introduced in the BIMs as substituents in the indole and furaldehyde moieties. Various commonly encountered biorenewable carboxylic acids were screened as catalysts for the acid-catalyzed transformation under organic solvent-free conditions. All the novel BIMs were characterized by spectroscopic techniques (FTIR, <sup>1</sup>H-NMR, <sup>13</sup>C-NMR) and elemental analysis. The reaction was optimized on the reaction temperature, duration, catalyst type, and catalyst loading. The gluconic acid aqueous solution (GAAS) showed the best catalytic activity for the transformation, affording satisfactory isolated yields (68–96%) of the targeted BIMs under optimized conditions. The GAAS catalyst was conveniently recovered from the reaction mixture and reused for four consecutive cycles without catastrophic loss in either mass or activity. Moreover, the antibacterial activities of the novel BIMs were studied on Gram-positive and Gram-negative bacterial strains, such as *Enterococcus faecalis* and *Pseudomonas syringae*.

Received 27th May 2024

Accepted 1st July 2024

DOI: 10.1039/d4ra03905j

rsc.li/rsc-advances

## 1. Introduction

Carbohydrate-derived 5-substituted-2-furaldehydes (SFLs) have attracted serious attention as biorenewable platform chemicals for synthesizing various classes of organic chemicals of commercial appeal.<sup>1–3</sup> The two most prominent members of biorenewable furaldehydes are furfural (FF) and 5-(hydroxymethyl)furfural (HMF), whereas the other SFLs are typically synthesized from these two chemicals by predominantly catalytic processes.<sup>4</sup> FF is produced by the acid-catalyzed dehydration of pentose sugars (*e.g.*, xylose) in the hemicellulose fraction of lignocellulosic biomass.<sup>4,5</sup> On the other hand, HMF is formed by the acid-catalyzed dehydration of hexoses (*e.g.*, glucose) in the cellulose and hemicellulose fractions.<sup>6</sup> The derivative chemistry of FF and HMF has expanded rapidly over the past decades, encompassing virtually all types of organic compounds and product classes.<sup>7,8</sup> FF is commonly used as

a substrate in various organic methodologies and catalytic organic transformations to demonstrate the broad substrate scope of the process.<sup>9</sup> The systematic study of biomass-derived SFLs as renewable substrates for synthesizing novel heterocyclic compounds has enormous scope but is relatively underexplored in the literature. The chemistry of heterocycles is one of the cornerstones of synthetic organic chemistry, and they are known for their remarkable biological and pharmacological properties.<sup>10,11</sup> The systematic synthesis of novel heterocyclic compounds starting from SFLs would allow access to hitherto unexplored molecules, study their physicochemical properties and biological activities, and explore their potential applications. We have recently reported the synthesis of novel heterocyclic compounds starting with SFLs as biorenewable reactants, using Morita–Baylis–Hillman, Biginelli, and Hantzsch reactions.<sup>12,13</sup> In this regard, bis(indolyl)methane (BIM) is a well-documented class of heterocycle with remarkable antimicrobial, antibacterial, antiviral, antifungal, anti-metastatic, analgesic, and anti-inflammatory activities.<sup>14–16</sup> BIMs are synthesized by the acid-catalyzed condensation between two indole (or 2-substituted indole) molecules with a suitable aldehyde under acid catalysis. Numerous catalysts and reaction media have been examined for the selective and high-yielding synthesis of BIMs with desired synthetic versatility, substrate scope, and process scalability. With increasing awareness about the sustainability and environmental impact of organic

<sup>a</sup>Department of Chemistry National Institute of Technology Karnataka (NITK) Surathkal, Mangalore 575025, India. E-mail: sdutta@nitk.edu.in

<sup>b</sup>Department of PG Studies and Research in Applied Botany, Kuvempu University, Jnanasahyadri, Shankaraghatta 577451, Karnataka, India

<sup>c</sup>Mechanical Engineering Department, College of Engineering, King Saud University, Riyadh 11421, Saudi Arabia

† Electronic supplementary information (ESI) available: FTIR, NMR (<sup>1</sup>H & <sup>13</sup>C), and elemental analysis data of the synthesized compounds. See DOI: <https://doi.org/10.1039/d4ra03905j>


transformations, new generations of effective and innocuous catalysts and reaction media are being developed for synthesizing BIMs.<sup>17,18</sup> Research has also been focused on using sustainable starting materials, reagents, and reaction auxiliaries sourced from renewable biomass to ensure leading to economic, social, and environmental advantages. A high-yielding synthesis of novel BIMs starting from SFLs under environmentally acceptable conditions will improve the economic feasibility of SFLs as sustainable chemical building blocks. Since increasing attention given to sustainability in the chemical industry, organic transformations have been performed in aqueous media or melt, avoiding the use of hazardous, volatile organic solvents.<sup>19–21</sup> Biogenic acids and their aqueous solutions have received immense interest as efficient catalysts and reaction media since they are renewable, eco-friendly, recoverable, and inexpensive.<sup>22–25</sup> Acetic acid, lactic acid, formic acid, oxalic acid, and gluconic acid aqueous solution (GAAS) are some of the most frequently used biomass-derived acid catalysts for acid-catalyzed organic transformations.<sup>26–28</sup> Interestingly, the synthesis of BIMs has already been attempted using carboxylic acids as catalysts. For example, itaconic acid has been used as a biorenewable carboxylic acid catalyst for the synthesis of BIMs starting from substituted benzaldehydes.<sup>29</sup> Gluconic acid is chemically stable, non-volatile, and is roughly ten times stronger acid ( $pK_a = 3.70$ ) than acetic acid.<sup>30</sup> Gluconic acid can be produced by the chemocatalytic or enzymatic oxidation of glucose or polymeric carbohydrates (*e.g.*, cellulose).<sup>31,32</sup> Herein, we report the production of novel BIMs by condensing indoles and bio-renewable SFLs using GAAS as an efficient, renewable, innocuous, and recyclable acid catalyst under organic solvent-free conditions (Scheme 1). The process has been optimized on various reaction parameters, such as temperature, duration, and catalyst loading, to ensure high selectivity and yield of the targeted BIMs under environmentally acceptable conditions.

The antibacterial activities of the novel BIMs towards Gram-positive and Gram-negative bacteria have also been investigated.

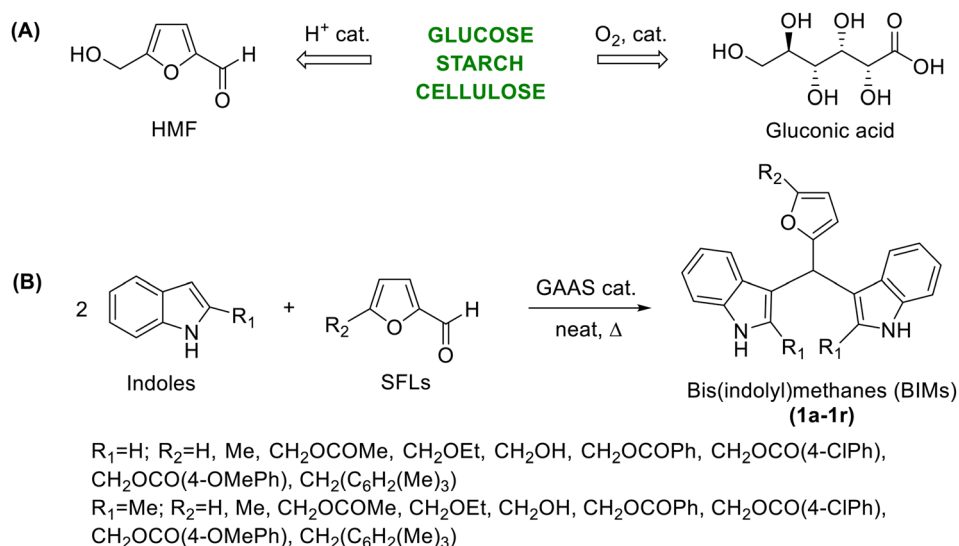
## 2. Experimental

### 2.1. Materials

Indole (99%), 2-methylindole (98%), furfural (99%), and mesitylene (99%) were purchased from Spectrochem Pvt. Ltd. 5-Methylfurfural (99%) was purchased from Sigma-Aldrich. 5-(Chloromethyl)furfural, 5-(hydroxymethyl)furfural, 5-(acetoxymethyl)furfural, 5-(ethoxymethyl)furfural, 5-(benzyloxymethyl)furfural, 5-(4-methoxybenzyloxymethyl)furfural, 5-(4-chlorobenzyloxymethyl)furfural, and 5-(mesitylmethyl)furfural were synthesized as per the reported literature.<sup>33,34</sup> Gluconic acid (50%, aq.) was purchased from TCI, Japan. Dimethyl sulfoxide (DMSO, 99%) was purchased from Himedia Laboratory, Mumbai, India. Thin-layer chromatography (TLC) plates, silica gel pre-coated on aluminium sheets, were purchased from Merck (TLC Silica Gel 60 F254).

### 2.2. Instrumentation

The synthesized BIMs were characterized by spectroscopic methods and elemental analysis. Fourier transform infrared (FTIR) spectra were collected using the ATR method in a Bruker Alpha II FTIR instrument equipped with zinc selenide (ZnSe) as the prism material. The compounds were dissolved in chloroform, and a thin film was made by evaporating a drop of the solution on the ATR counter. Each FTIR spectrum was collected by taking 24 scans at a scanning speed of 4 scans per second within the spectral range of 500–4000  $\text{cm}^{-1}$ . For nuclear magnetic resonance (NMR) spectroscopy, the  $^1\text{H}$ -NMR spectra were collected in a Bruker NanoBay® NMR instrument at the operating radio frequency of 400 MHz. The  $^{13}\text{C}$ -NMR spectra were recorded in the same instrument at the frequency of 100



**Scheme 1** (A) Biorenewable synthesis of HMF and gluconic acid from carbohydrates, and (B) GAAS-catalyzed synthesis of novel BIMs starting from SFLs and indoles.



MHz (calculated). Elemental analyses of the synthesized novel compounds were collected using Elementar, Germany (Model: vario MICRO select). The melting point of the bis(indolyl) methanes was measured in the Stuart SMP3 digital melting point apparatus.

### 2.3. Synthetic procedure

**2.3.1. Synthesis of 3,3'-((5-methylfuran-2-yl)methylene) bis(1*H*-indole) (**1b**).** MF (0.250 g, 2.27 mmol), indole (0.531 g, 4.53 mmol), and GAAS (0.445 g, 1.13 mmol, 50 mol%) were charged into a round-bottomed flask (25 mL) equipped with a water-jacketed reflux condenser. The flask was placed in a preheated (80 °C) oil bath and magnetically stirred for 6 h. The reaction progress was monitored by thin-layer chromatography for the disappearance of MF. After the reaction, the reaction mixture was cooled down to room temperature and quenched in ice-cold water. The aqueous suspension was filtered, washed with hot pet ether, and dried in air. The crude product was dissolved in ethanol, decolorized with activated carbon, filtered under vacuum, and evaporated in a rotary evaporator under reduced pressure to get purified **1b** (0.652 g, 88%) as a faintly red solid.

### 2.4. Antibacterial studies

The antibacterial activity of the compounds was assessed using the agar well diffusion method. The synthesized compounds were tested for their potential antibacterial activity against selected clinical and pathogenic bacterial strains (cultures were procured from the Institute of Microbial Technology, Chandigarh, India), Gram-positive bacteria- *Enterococcus faecalis* (MTCC 439), *Staphylococcus aureus* (MTCC 902), Gram-negative bacteria- *Klebsiella pneumoniae* (MTCC 1559), and *Pseudomonas syringae* (MTCC-1604) by agar well diffusion method.<sup>35</sup> For testing activity on the bacterial strains, Ciprofloxacin (Ciprodac 250, CADILA Pharmaceuticals Limited), a broad-spectrum commercial antibiotic, was used as the positive control, and dimethyl sulfoxide was used as the negative control. Bacterial strains were cultured in the nutrient agar broth. The test compounds (10 mg) were dissolved separately in dimethyl sulfoxide (1000 µL) and diluted to three different concentrations, specifically, 100% (10 mg mL<sup>-1</sup>), 50% (5 mg mL<sup>-1</sup>), and 25% (2.5 mg mL<sup>-1</sup>). The zone of inhibition (ZI) data is the average of three replicates and data represented in standard deviation (SD). The bacterial suspension was swabbed on the solidified agar media. Wells were made on the solid agar medium using a sterile cork borer (5 mm diameter), and 20 µL of the test sample, standard solution of Ciprofloxacin, or the solvent was added to each well and incubated at 37 °C for 24 h. Petri plates were observed to measure the ZI (diameter in mm) for evaluating the antibacterial activity of the synthesized BIMs.<sup>36</sup>

## 3. Results and discussion

Initially, bis(indolyl)methane **1b** was synthesized by mixing 5-methylfurfural (MF) and indole in a 1:2 molar ratio and

magnetically stirring the mixture at elevated temperatures. The reaction progress was monitored by using TLC for the disappearance of MF. The control reaction, performed without a catalyst, resulted in a 20% yield of **1b** after 24 h. The low yield was due to slow kinetics and low conversion of MF at room temperature. When the temperature was raised to 80 °C, the reaction gave a 60% yield of **1b** after 12 h. However, the reaction remained incomplete, and partial decomposition of MF was observed. The synthesis of **1b** was then attempted using the aqueous solution of different biogenic acids as catalysts. When the reaction was carried out at 80 °C using roughly 1:2 molar ratio of MF and indole in the presence of 50 mol% of GAAS (50%, aq.), an 88% isolated yield of **1b** was obtained. Table 1 shows the influence of various biorenewable carboxylic acids in the aqueous solution as an acid catalyst for synthesizing **1b**. The reaction temperature was fixed at 80 °C, and the reaction was continued till the complete conversion of MF. Three carboxylic acids, namely, acetic acid (entry 2), GAAS (entry 4), and lactic acid (entry 5), afforded high isolated yields (>80%) of the targeted product **1b**. Lactic acid showed particularly interesting catalytic activity, affording an 84% yield of **1b** after 1 h at 80 °C. However, the GAAS catalyst provided higher isolated yields (4–8%) of the targeted BIMs from other SFLs under optimized conditions. Moreover, multiple spots were observed on the TLC plate when lactic acid was used as the catalyst, requiring chromatographic purification of the products. No direct relationship between the p*K*<sub>a</sub> of the acid catalyst and its activity (or selectivity) was apparent. 2,5-Furandicarboxylic acid gave only a 54% yield of **1b**, possibly due to the low solubility of the acid catalyst in the aqueous medium. Levulinic acid (entry 7) and oxalic acid (entry 9) gave 78% and 76% yields of **1b**, respectively. Formic acid (entry 3) afforded a 68% yield of **1b** after 3 h at 80 °C, whereas succinic acid (entry 6) gave a 60% yield after 2 h reaction. GAAS was found to be the most efficient catalyst, providing an 88% isolated yield of **1b** after 6 h at 80 °C (entry 4). Therefore, further reaction optimizations were performed using GAAS as the catalyst of choice. The transformation was then optimized on various other reaction parameters, such as reaction temperature, catalyst loading, and reaction duration. Initially, the effect of reaction temperature was studied since it affects the reaction kinetics, product selectivity, and stability of

Table 1 The synthesis of bis(indolyl)methane **1b** from 5-methylfurfural using various biogenic acids as catalysts<sup>a</sup>

Entry	Catalyst	Time (h)	Yield (%)
1	No catalyst	12	60
2	Acetic acid	2.5	81
3	Formic acid	3	68
4	GAAS	6	88
5	Lactic acid	1	84
6	Succinic acid	2	60
7	Levulinic acid	2	78
8	2,5-Furandicarboxylic acid	7	54
9	Oxalic acid	2	76

<sup>a</sup> Reaction conditions: MF (0.250 g, 2.27 mmol), indole (0.531 g, 4.53 mmol), catalyst (50 wt% aqueous solution, 50 mol%), 80 °C.

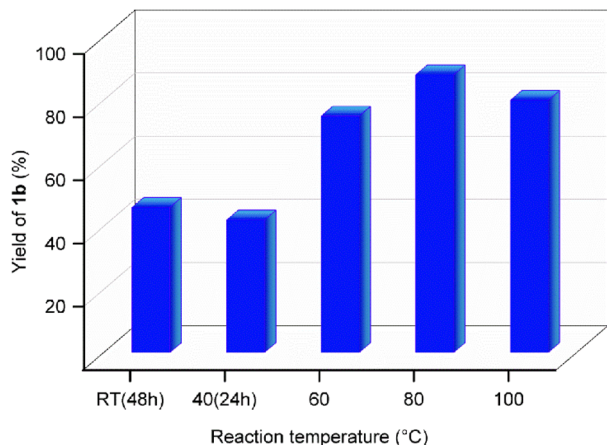


Fig. 1 The effect of reaction temperature on the isolated yield of bis(indolyl)methane **1b**. Reaction conditions: MF (0.250 g, 2.27 mmol), indole (0.531 g, 4.53 mmol), GAAS (50 mol%).

reactants, products, and catalysts. When the reaction was performed at RT with 50 mol% GAAS catalyst, the yield of **1b** reached 46% after 48 h (Fig. 1). The low yield was due to slow kinetics and incomplete conversion of MF. When the temperature was slightly elevated to 40 °C, the kinetics got faster, and a 40% yield of **1b** was obtained within 24 h. Increasing the temperature to 60 °C gave a 72% yield of **1b** after 6 h of reaction. The yield of **1b** reached maximum at 88% when the reaction was performed for 6 h at 80 °C. However, further increasing the reaction temperature to 100 °C lowered the yield of **1b** to 76% due to partial decomposition of MF in aqueous acid at elevated temperature. Therefore, 80 °C was considered the optimum reaction temperature for synthesizing novel BIMs from SFLs. Scaling up the reaction with 2 g of MF gave a 90% isolated yield of **1b** under optimized conditions (*i.e.*, 80 °C, 6 h, 50 mol% GAAS). The effect of the loading of the GAAS catalyst on the isolated yield of **1b** was studied next. When the loading of GAAS (with respect to the mmol of MF used) was decreased to 25 mol%, a 74% yield of **1b** was obtained after 6 h of reaction at 80 °C. The lower yield was due to incomplete conversion of MF due to slower kinetics. However, using an excess catalyst (1 mL of GAAS for 0.250 g of MF) also marginally decreased the yield of **1b** (compared to that using 50 mol% GAAS catalyst) due to the accelerated decomposition of MF in the aqueous acid.

The effect of reaction duration on the yield of **1b** was studied next by keeping the reaction temperature and the loading of the GAAS catalyst at their optimized values (Fig. 2). A duration of 4 h gave only a 65% isolated yield of **1b** due to incomplete conversion of MF. Increasing the reaction duration to 6 h gave an 88% yield of **1b**, which remained the same even after 8 h of reaction. Extending the reaction duration to 10 h marginally decreased the yield of **1b** to 84% due to partial decomposition of **1b** in the aqueous acid at elevated temperature. Recyclability of the catalyst is a crucial factor in organic transformation for favorable green metrics and process economy. Even though GAAS is relatively inexpensive, non-toxic, and sustainably produced from carbohydrates, the recyclability of the GAAS catalyst was explored.

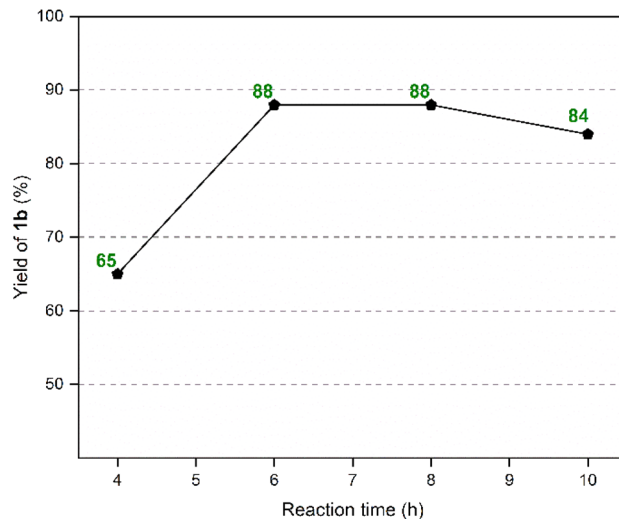


Fig. 2 Effect of reaction duration on the isolated yield of **1b**. Reaction conditions: MF (0.250 g, 2.27 mmol), indole (0.531 g, 4.53 mmol), GAAS (50 mol%), 80 °C.

Recyclability of the GAAS catalyst was tested under optimized reaction conditions (*i.e.*, 80 °C, 6 h, 50 mol% GAAS). After the reaction, the mixture was cooled to room temperature, poured into crushed ice, and the product was separated by vacuum filtration. The aqueous layer was evaporated under reduced pressure to recover the catalyst. The recycled GAAS catalyst showed good catalytic activity up to four cycles with only a marginal dip in activity (Fig. 3). The slight dip in the catalytic activity of the GAAS catalyst could result from the mass loss of gluconic acid during recycling or its partial lactonization during the evaporation of excess water.

The optimized reaction conditions for **1b** were applied to synthesize BIMs (**1a–1r**). The molecular structure, yield, and antibacterial activity of BIMs **1a–1i**, produced by reacting SFLs with two equivalents of indole in the presence of 50 mol% GAAS

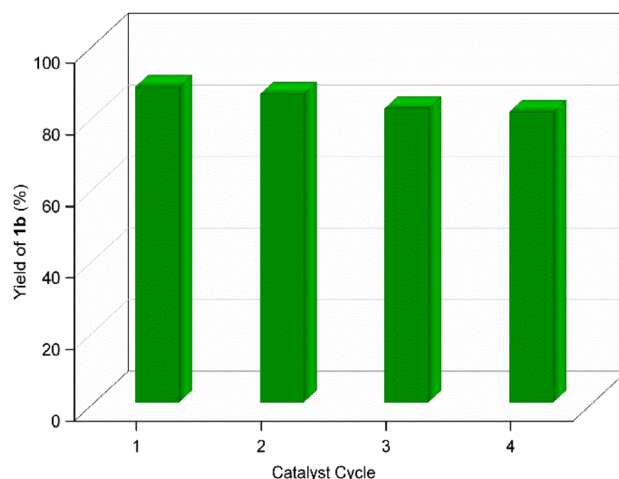


Fig. 3 Recyclability study of the GAAS catalyst for synthesizing bis(indolyl)methane **1b**. Reaction conditions: MF (0.250 g, 2.27 mmol), indole (0.531 g, 4.53 mmol), GAAS (0.445 g, 50 mol%), 80 °C, 6 h.





**Table 2** Synthesis of novel bis(indolyl)methanes starting from biorenewable 5-substituted-2-furaldehydes and indole and their antibacterial activities<sup>a</sup>

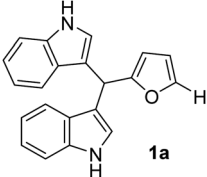
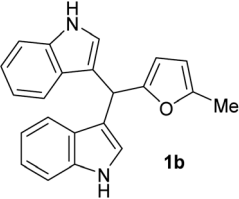
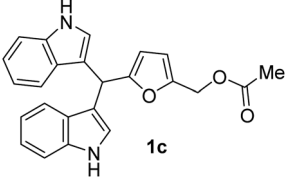
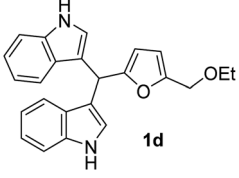
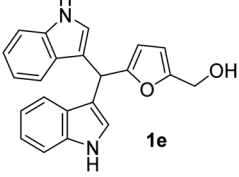
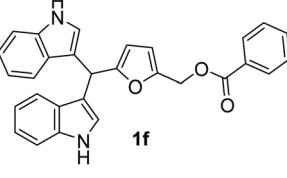
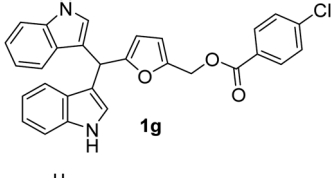
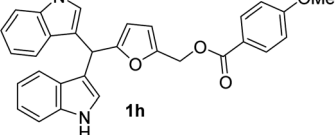
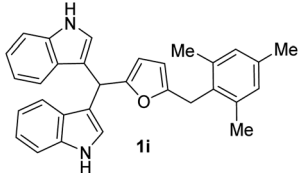
Entry	Structure & code	Time (h)	Yield (%)	Antibacterial activity		
				Conc. <sup>c</sup> (%)	ZI (mean $\pm$ SD in mm)	
					Ef	Ps
1		6	96	100	9 $\pm$ 0.57	0
				50	6 $\pm$ 0.12	0
				25	3.5 $\pm$ 0.57	0
2		6	88	100	7 $\pm$ 0.57	9 $\pm$ 0.57
				50	6 $\pm$ 0.21	6.5 $\pm$ 0.12
				25	2.5 $\pm$ 1	3.8 $\pm$ 0.57
3		1.5	90	100	7 $\pm$ 1	7 $\pm$ 0.57
				50	5 $\pm$ 0.57	4 $\pm$ 0.57
				25	2.5 $\pm$ 0.23	2 $\pm$ 0.23
4 <sup>b</sup>		1.5	82	100	0	0
				50	0	0
				25	0	0
5 <sup>b</sup>		3	68	100	12 $\pm$ 0.22	13 $\pm$ 0.23
				50	8 $\pm$ 0.57	11 $\pm$ 0.57
				25	6 $\pm$ 0.32	8 $\pm$ 0.57
6 <sup>b</sup>		8	88	100	12 $\pm$ 0.57	10 $\pm$ 0.12
				50	10 $\pm$ 0.21	8 $\pm$ 0.57
				25	8 $\pm$ 0.57	6 $\pm$ 0.32
7		5	85	100	13 $\pm$ 0.57	12 $\pm$ 0.57
				50	10 $\pm$ 0.52	10 $\pm$ 0.22
				25	8 $\pm$ 0.12	8 $\pm$ 0.11
8 <sup>b</sup>		8	68	100	0	0
				50	0	0
				25	0	0



Table 2 (Contd.)

Entry	Structure & code	Time (h)	Yield (%)	Conc. <sup>c</sup> (%)	Antibacterial activity	
					ZI (mean $\pm$ SD in mm)	
					Ef	Ps
9	 1i	12	78	100	14 $\pm$ 0.23	15 $\pm$ 0.57
				50	10 $\pm$ 0.57	10 $\pm$ 0.15
				25	7 $\pm$ 0.17	8 $\pm$ 0.57

<sup>a</sup> Reaction conditions: SFLs (5.21 mmol), indole (10.42 mmol, 2 equiv.), GAAS catalyst (50 mol% of SFL), 80 °C. <sup>b</sup> 60 °C, 25 mol% GAAS.

<sup>c</sup> Concentrations (100% = 10 mg mL<sup>-1</sup>, 50% = 5 mg mL<sup>-1</sup>, 25% = 2.5 mg mL<sup>-1</sup>). The antibacterial activity of the standard Ciprofloxacin is 28.1  $\pm$  0.57 mm for Ef and 26.3  $\pm$  0.57 mm for Ps (at 100% conc.).

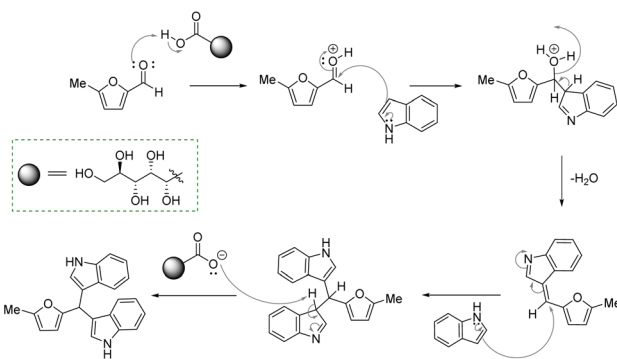


Fig. 4 The proposed mechanism of forming **1b** starting from indole and MF using GAAS as the catalyst.

catalyst, are listed in Table 2. All the SFLs afforded good to excellent isolated yields of the corresponding BIM. HMF and 5-(4-methoxybenzyloxymethyl)furfural gave relatively lower yields (*i.e.*, 68%) of the corresponding BIMs (**1e** & **1h**) (entry 5 & 8, Table 2). The lower yield in the case of HMF was due to the inherent instability of HMF in aqueous acid. When the required amount of HMF was used at a stretch at 60 °C, only a 60% yield of **1e** was obtained. The yield of **1e** improved to 68% when HMF was added slowly in portions to the preheated mixture of indole and GAAS. Increasing the temperature to 80 °C or increasing the GAAS catalyst loading to 50 mol% accelerated the reaction, but the selectivity towards **1e** was low due to the partial decomposition of HMF. The relatively low yield of **1h** was due to the

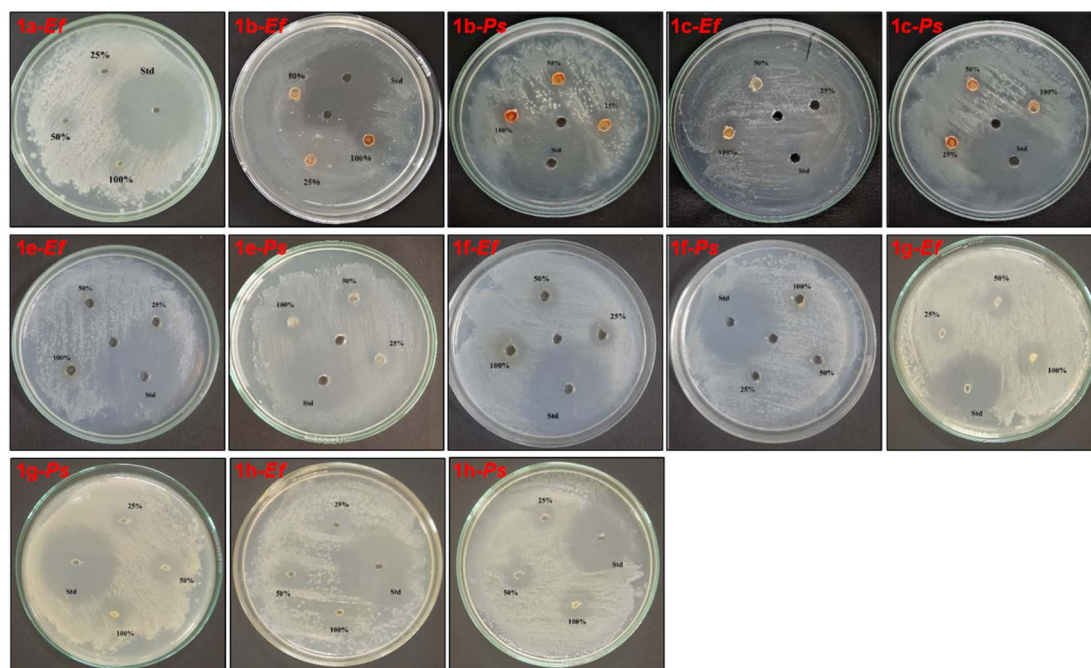


Fig. 5 Photographic images of the Petri plates for studying antibacterial activities of BIMs **1j**–**1r** against the bacterial strains Ef and Ps.



Table 3 Synthesis of BIMs from SFLs and 2-methylindole<sup>a</sup>

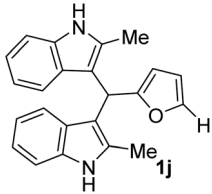
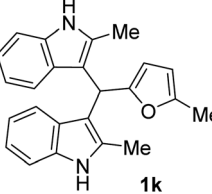
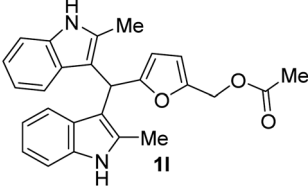
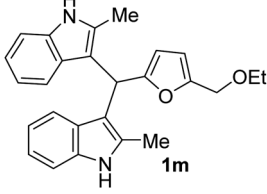
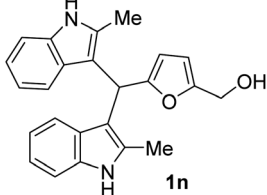
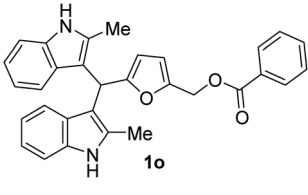
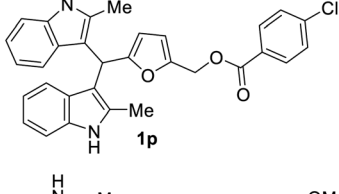
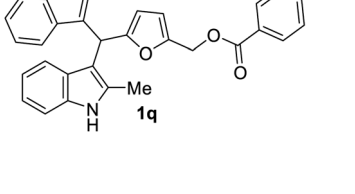
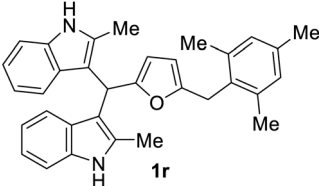
Entry	Structure & code	Time (min)	Yield (%)	Conc. (%)	Zone of inhibition (mean $\pm$ SD in mm)	
					Sa	Ps
1		20	95	100	18 $\pm$ 0.57	14 $\pm$ 0.57
				50	16 $\pm$ 0.1	13 $\pm$ 0.22
				25	14 $\pm$ 0.57	12 $\pm$ 0.57
2		20	94	100	15 $\pm$ 1	14 $\pm$ 0.57
				50	14 $\pm$ 0.57	12 $\pm$ 0.32
				25	12 $\pm$ 0.52	8 $\pm$ 0.57
3		45	90	100	16 $\pm$ 0.57	0
				50	14 $\pm$ 1	0
				25	13 $\pm$ 0.23	0
4		90	78	100	0	6 $\pm$ 0.23
				50	0	4 $\pm$ 0.32
				25	0	2 $\pm$ 1
5		90	76	100	15 $\pm$ 0.57	12 $\pm$ 0.23
				50	10 $\pm$ 1	10 $\pm$ 0.32
				25	6 $\pm$ 0.23	6 $\pm$ 1
6		90	90	100	0	6 $\pm$ 0.57
				50	0	4 $\pm$ 0.3
				25	0	2 $\pm$ 0.23
7		90	84	100	19 $\pm$ 1	10 $\pm$ 0.57
				50	17 $\pm$ 0.3	6 $\pm$ 0.23
				25	16 $\pm$ 0.23	4 $\pm$ 0.57
8		90	86	100	18 $\pm$ 0.57	12 $\pm$ 0.57
				50	15 $\pm$ 0.57	10 $\pm$ 0.32
				25	11 $\pm$ 0.23	7 $\pm$ 0.57



Table 3 (Contd.)

Entry	Structure & code	Time (min)	Yield (%)	Conc. (%)	Zone of inhibition (mean $\pm$ SD in mm)	
					Sa	Ps
9	 1r	90	80	100	12 $\pm$ 0.57	0
				50	10 $\pm$ 1	0
				25	8 $\pm$ 0.57	0

<sup>a</sup> Reaction conditions: SFLs (5.21 mmol), 2-methylindole (10.42 mmol, 2 equiv.), GAAS catalyst (25 mol% of SFL). The antibacterial activity of the standard Ciprofloxacin was 28.1  $\pm$  0.57 mm for Sa and 26.3  $\pm$  0.57 mm for Ps (at 100% conc.).

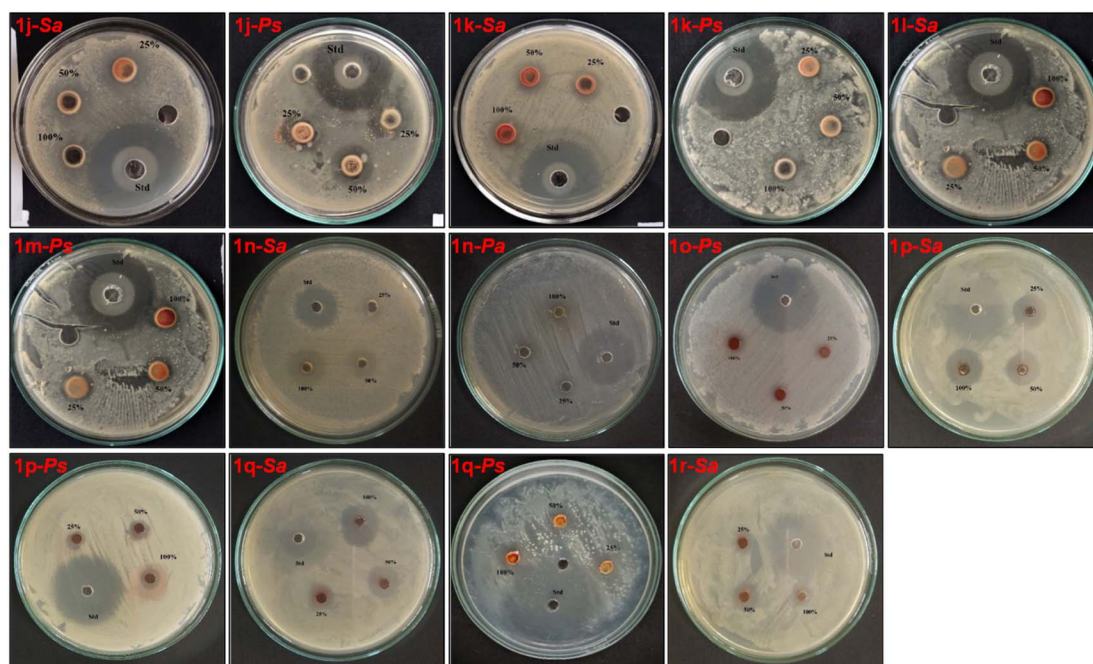


Fig. 6 Photographs of the Petri plates for studying antibacterial activities of BIMs 1j–1r against the bacterial strains Sa and Ps.

partial hydrolysis of the ester group. The reaction for **1h** was also performed at a lower reaction temperature and decreased catalyst loading (*i.e.*, 60 °C, 25 mol% GAAS) since higher temperature and higher loading of the GAAS catalyst led to increased hydrolysis of the ester group. A plausible mechanism for the synthesis of **1b** from MF and indole has been proposed (Fig. 4). The carbonyl oxygen atom in furfural is first activated by the carboxylic acid functionality in GAAS. The sequential nucleophilic attack by two indole molecules from the C-3 position followed by rearomatization leads to **1b**.

The antibacterial activity of BIMs **1a–1i** (from indole) and BIMs **1j–1r** (from 2-methylindole) were assessed by the agar well

diffusion method. The growth inhibitory effects of the compounds were evaluated against Gram-positive strains *Staphylococcus aureus* (Sa) and *Enterococcus faecalis* (Ef) and Gram-negative bacteria strain *Pseudomonas syringae* (Ps). The antibacterial effect was analyzed by considering the diameter of the inhibition zone formed around the well. The results of the antibacterial activity of BIMs **1a–1i** are summarized in Table 2. No antibacterial activity was observed for compounds **1d** and **1h**. Weak antibacterial activity was observed for **1a–1c** towards Ef and Ps. Fig. 5 shows the photographic images of the Petri plates after the incubation (37 °C, 24 h), containing bacterial strains (Ef & Ps) for studying the ZI of the synthesized BIMs **1a–**





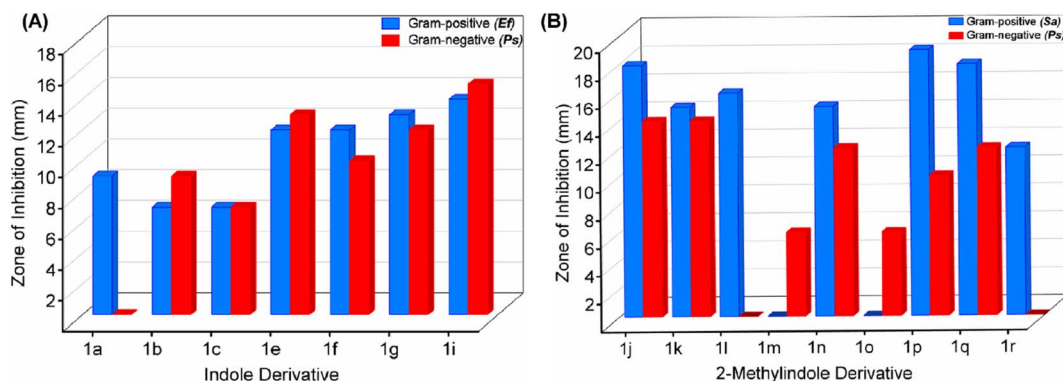


Fig. 7 Comparison of antibacterial activities on Gram-positive and Gram-negative bacterial strains by BIMs synthesized from (A) indole and (B) 2-methylindole.

**1i** at different concentrations against the standard antibiotic Ciprofloxacin.

The BIMs **1j–1r** were produced in satisfactory isolated yields (76–95%) starting from SFLs and 2-methylindole. 2-Methylindole was found to be significantly more reactive than indole for synthesizing BIMs. The introduction of a methyl group increased the nucleophilicity of 2-methylindole compared to indole. The yield of **1n** (entry 5, Table 3) from HMF and 2-methylindole was 76%, compared to only 68% for **1e** (entry 5, Table 2) from HMF and indole. Moreover, the synthesis of **1n** took only 1.5 h, whereas **1e** took 3 h to complete. The result can be explained by the faster kinetics for **1n** that minimized the scope for HMF degradation. The synthesis of other BIMs from 2-methylindole was significantly faster than those synthesized from indole.

The BIMs synthesized from 2-methylindole (*i.e.*, **1j–1r**) showed good antibacterial activity compared to those obtained from indole (*i.e.*, **1a–1i**). BIMs **1j–1r** showed more aggression towards Gram-positive bacterial strain Sa rather than Ps. The antibacterial resistance of Gram-negative bacteria compared to Gram-positive bacteria could be attributed to the different cell wall structure of the two types. Gram-negative bacteria have an effective permeability barrier composed of a thin peptidoglycan and an outer membrane, which limits the penetration of the test compound. On the other hand, the cell wall of Gram-positive bacteria Sa is made up of only a single thick layer of peptidoglycan, making it more susceptible to antibacterial compounds like BIMs.

The novel and biorenewable BIMs, such as **1g**, **1q**, **1j**, and **1l**, showed significant antibacterial effects towards Gram-positive bacterial strain Sa with the ZI value of  $19 \pm 1$  mm,  $18 \pm 0.57$  mm,  $18 \pm 0.57$  mm, and  $16 \pm 0.57$  mm, respectively, at the concentration of  $10 \text{ mg mL}^{-1}$ . The BIMs synthesized from indole, such as **1h**, **1e**, and **1g**, showed moderate antibacterial effect against Gram-negative bacteria Ps with the ZI value of  $15 \pm 0.57$  mm,  $13 \pm 0.23$  mm, and  $12 \pm 0.57$  mm, respectively. The ZI values of the same compounds for the Gram-positive Sa resulted in ZI values of  $14 \pm 0.23$  mm,  $12 \pm 0.22$  mm, and  $13 \pm 0.57$  mm, respectively, at the concentration of  $10 \text{ mg mL}^{-1}$ . All other BIMs showed low to moderate antibacterial activity towards the selected bacterial strains. Ciprofloxacin, the

standard antibiotic chosen for this study, showed ZI values of  $28.1 \pm 0.57$  mm and  $26.3 \pm 0.57$  mm against Sa and Ps, respectively. Gram-negative bacteria are typically more resistant to antibiotic compounds than Gram-positive bacteria.<sup>37</sup> Colony inhibition in the bacterial strains might be brought about by the suppression of DNA or protein synthesizers that damage the integrity of cell membranes leading to cell death.<sup>38</sup> The inhibitory effect of BIMs against pathogenic bacterial strains could be associated with active functional groups (*i.e.*, indole, substituents on the furan ring) present in the compounds.

Fig. 6 shows the photographs of the Petri plates after the incubation ( $37^\circ\text{C}$ , 24 h), containing bacterial strains Sa and Ps, for studying the ZI of the synthesized BIMs **1j–1r** at different concentrations against the standard antibiotic Ciprofloxacin.

Interestingly, BIMs **1a–1i**, synthesized from indole and SFLs, show comparable or slightly better antibacterial activity towards Gram-negative Ps compared to Gram-positive strain Ef (Fig. 7a). However, in the case of **1a**, no activity was observed on Ef. The compound **1i**, produced by reacting 5-(mesitylmethyl)furfural with indole, showed promising antibiotic properties on both Ef and Ps. The ZI was around 50% of the standard antibiotic Ciprofloxacin used in this study. In the case of BIMs **1j–1r**, produced by reacting SFLs with 2-methylindole, showed significantly better antibacterial activity on Gram-positive bacteria Sa compared to Ps (Fig. 7b). The compounds **1j** and **1p** showed the best antibacterial activity on Sa with ZI of  $19 \pm 1$  mm and  $18 \pm 0.57$  mm, respectively, compared to  $28 \pm 0.57$  mm for Ciprofloxacin.

## 4. Conclusions

In conclusion, a general protocol has been developed for synthesizing novel BIMs from carbohydrate-derived SFLs. A total of eighteen BIMs has been synthesized in good to excellent isolated yields under optimized reaction conditions using GAAS as an efficient, recyclable, and sustainable catalyst. The structural features in the synthesized BIMs were introduced as substituents in the furaldehyde and indole moieties. Moreover, antibacterial activities of the novel BIMs were studied in



Gram-positive and Gram-negative bacterial strains. Some BIMs showed promising antibacterial activity on both bacterial strains in comparison with the standard antibiotic Ciprofloxacin. The straightforward and high-yielding synthesis of BIMs starting from biorenewable SFLs will encourage synthesizing other crucial heterocyclic structures from the latter.

## Data availability

The data supporting this article have been included as part of the ESI.†

## Author contributions

Prajwal Naik C: experimental work and design of methodology. Ashoka G. B.: experimental work and reviewing the draft. Asiful H. Seikh: funding acquisition and reviewing the draft. Saikat Dutta: conceptualization, supervision, and writing the original manuscript. The submitted version of this manuscript was checked and approved by all authors.

## Conflicts of interest

The authors declare no competing interest.

## Acknowledgements

The authors thank the Central Research Facility (CRF) at NITK, Surathkal, for recording the Nuclear Magnetic Resonance (NMR) spectroscopy data. Raman Research Institute, Bangalore, is acknowledged for their assistance in collecting the Elemental Analysis data. The authors acknowledge the Researchers Supporting Project number (RSP2024R373), King Saud University, Riyadh, Saudi Arabia. SD thanks Science and Engineering Research Board (SERB), India, for approving research projects under the Core Research Grant (CRG) scheme (File no. CRG/2021/001084 and CRG/2022/009346).

## References

- 1 X. Zhang, S. Xu, Q. Li, G. Zhou and H. Xia, *RSC Adv.*, 2021, **11**, 27042–27058.
- 2 X. Kong, Y. Zhu, Z. Fang, J. A. Kozinski, I. S. Butler, L. Xu, H. Song and X. Wei, *Green Chem.*, 2018, **20**, 3657–3682.
- 3 S. Dutta, *Biomass Convers. Biorefin.*, 2023, **13**, 10361–10386.
- 4 H. N. Anchan and S. Dutta, *Biomass Convers. Biorefin.*, 2023, **13**, 2571–2593.
- 5 X. Li, P. Jia and T. Wang, *ACS Catal.*, 2016, **6**, 7621–7640.
- 6 S. P. Teong, G. Yi and Y. Zhang, *Green Chem.*, 2014, **16**, 2015–2026.
- 7 W. Fan, C. Verrier, Y. Queneau and F. Popowycz, *Curr. Org. Synth.*, 2019, **16**, 583–614.
- 8 R. Mariscal, P. Maireles-Torres, M. Ojeda, I. Sádaba and M. López Granados, *Energy Environ. Sci.*, 2016, **9**, 1144–1189.
- 9 A. M. Abdella, A. M. Abdelmoniem, I. A. Abdelhamid and A. H. M. Elwaby, *J. Heterocycl. Chem.*, 2020, **57**, 1476–1523.
- 10 E. Kabir and M. Uzzaman, *Results Chem.*, 2022, **4**, 100606.
- 11 A. P. Taylor, R. P. Robinson, Y. M. Fobian, D. C. Blakemore, L. H. Jones and O. Fadeyi, *Org. Biomol. Chem.*, 2016, **14**, 6611–6637.
- 12 H. N. Anchan and S. Dutta, *ChemistrySelect*, 2023, **8**, e202300264.
- 13 N. S. Bhat, M. Kumari, P. Naik C, S. S. Mal and S. Dutta, *ChemistrySelect*, 2023, **8**, e202301782.
- 14 A. Singh, G. Kaur and B. Banerjee, *Curr. Org. Chem.*, 2020, **24**, 583–621.
- 15 H. Gong and Z. Xie, *Chin. J. Org. Chem.*, 2012, **32**, 1195–1207.
- 16 M. Shyamsundar, S. Z. M. Shamshuddin, V. T. Vasanth and T. E. Mohankumar, *J. Porous Mater.*, 2017, **24**, 1003–1011.
- 17 K. A. Chavan, M. Shukla, A. N. S. Chauhan, S. Maji, G. Mali, S. Bhattacharyya and R. D. Erande, *ACS Omega*, 2022, **7**, 10438–10446.
- 18 J. Banothu, R. Gali, R. Velpula, R. Bavantula and P. A. Crooks, *ISRN Org. Chem.*, 2013, **2013**, 616932.
- 19 D. K. Romney, F. H. Arnold, B. H. Lipshutz and C.-J. Li, *J. Org. Chem.*, 2018, **83**, 7319–7322.
- 20 C.-J. Li, *Chem. Rev.*, 2005, **105**, 3095–3166.
- 21 K. Tanaka and F. Toda, *Chem. Rev.*, 2000, **100**, 1025–1074.
- 22 A. P. Sarkate, J. N. Sangshetti, N. B. Dharbale, A. P. Sarkate, P. S. Wakte and D. B. Shinde, *J. Chil. Chem. Soc.*, 2013, **58**, 2200–2203.
- 23 M. Dabiri, M. Baghbanzadeh and M. S. Nikcheh, *Monatsh. Chem.*, 2007, **138**, 1249–1252.
- 24 M. Kangani, N. Hazeri, A. Yazdani-Elah-Abadi and M.-T. Maghsoodlou, *Polycyclic Aromat. Compd.*, 2018, **38**, 322–328.
- 25 H. Y. Lim and A. V. Dolzhenko, *Sustainable Chem. Pharm.*, 2021, **21**, 100443.
- 26 X. Liu, S. Li, Y. Liu and Y. Cao, *Chin. J. Catal.*, 2015, **36**, 1461–1475.
- 27 J. Kim, Y.-M. Kim, V. R. Lebaka and Y.-J. Wee, *Fermentation*, 2022, **8**, 609.
- 28 K. Gopalaiah, *Synlett*, 2004, **2004**, 2838–2839.
- 29 S. B. Kasar and S. R. Thopate, *Curr. Org. Synth.*, 2018, **15**, 110–115.
- 30 Y. Ma, B. Li, X. Zhang, C. Wang and W. Chen, *Front. Bioeng. Biotechnol.*, 2022, **10**, 864787.
- 31 H. Zhang, N. Li, X. Pan, S. Wu and J. Xie, *ACS Sustainable Chem. Eng.*, 2017, **5**, 4066–4072.
- 32 J. F. Kornecki, D. Carballares, P. W. Tardioli, R. C. Rodrigues, Á. Berenguer-Murcia, A. R. Alcántara and R. Fernandez-Lafuente, *Catal. Sci. Technol.*, 2020, **10**, 5740–5771.
- 33 N. S. Bhat, A. K. Yadav, M. Karmakar, A. Thakur, S. S. Mal and S. Dutta, *ACS Omega*, 2023, **8**, 8119–8124.
- 34 N. S. Bhat, S. L. Hegde, S. Dutta and P. Sudarsanam, *ACS Sustainable Chem. Eng.*, 2022, **10**, 5803–5809.
- 35 D. Rekha and M. B. Shivanna, *Int. J. Curr. Microbiol. Appl. Sci.*, 2014, **3**, 573–591.
- 36 R. Nischitha and M. B. Shivanna, *3 Biotech*, 2021, **11**, 53.
- 37 B. Biswas, K. Rogers, F. McLaughlin, D. Daniels and A. Yadav, *Int. J. Microbiol.*, 2013, **2013**, 746165.
- 38 T. K. George, A. Joy, K. Divya and M. S. Jisha, *Microb. Pathog.*, 2019, **131**, 87–97.

